Clay Minerals, (2016) **51**, 707–714

EPR spectra of a new radiation-induced paramagnetic centre in kaolins

BERNARD A. GOODMAN[1,2,*], NIRAMON WORASITH[3] AND WEN DENG[1]

[1] *College of Physical Science & Engineering, Guangxi University, Nanning, 530004 Guangxi, China*
[2] *State Key Laboratory for Conservation and Utilization of Subtropical Agro-Bioresources, Guangxi University, Nanning, 530004 Guangxi, China*
[3] *Department of Chemistry, Faculty of Science and Technology, Rajamangala University of Technology Krungthep, 2 Nang Lin Chi Road, Soi Suan Plu, Sathorn, Bangkok, Thailand*

(*Received 3 November 2015; revised 18 July 2016; Editor: George Christidis*)

ABSTRACT: The EPR spectrum of a previously unreported paramagnetic centre formed in kaolin minerals by exposure to γ radiation is described. This centre, which is referred to here as the 'C-centre', was seen initially during an investigation of the radiation dose response of the EPR signal in the natural Lampang kaolin from northern Thailand, and its EPR properties are now presented for a purified sample from this material. They suggest a paramagnetic centre with rhombic symmetry based on O^- associated with a single ^{27}Al atom. Computer simulations suggest spin Hamiltonian parameters of $g_1 = 1.976$, $g_3 = 2.0417$ and $A(^{27}Al) = 2.10$ mT, with $g_2 \approx 2.01$. This C-centre was also seen as a minor radiation-induced component in both crude and purified Ranong kaolin samples, along with a stronger signal from the B-centre radical. It seems to be associated with the kaolinite component, but was lost on annealing to 300°C after which only the signal from the A-centre was visible.

KEYWORDS: kaolinite, free radical, γ radiation, ^{27}Al hyperfine structure.

Natural kaolin samples usually contain paramagnetic centres, either from transition metal ions or stable free radicals, that can be detected by electron paramagnetic resonance (EPR) spectroscopy; the diversity of their EPR spectra has been reviewed by Hall (1980), Muller & Calas (1993), and more recently by Allard *et al.* (2012). Three distinct radiation-induced free-radical EPR signals have been reported and these are generally referred to as the A-, A′-, and B-centres. Each is associated with an O^- defect in the oxygen framework of the kaolin minerals, and the different EPR spectra correspond to different structural sites for these defects as described by Allard & Calas (2009). The A-centre is associated with oxygen atoms that link the octahedral and tetrahedral sheets, and occurs at the boundaries of clusters of trioctahedral cells in the normal dioctahedral structure (Cuttler, 1980). Its EPR spectrum is characterized by an anisotropic signal with $g_{//} \approx 2.050$ and $g_{\perp} \approx 2.007$, usually with no evidence of hyperfine structure (hfs) (from interaction of the unpaired electron with a nucleus with non-zero spin). The A′-centre also has an anisotropic EPR signal without hfs, but with a smaller $g_{/}$ -value, of ~2.040, than that of the A-centre; it is considered to be located on the surface of the tetrahedral sheet (Lombardi *et al.*, 2002). In contrast, the B-centre contains extensive ^{27}Al hfs of ~0.76 mT, and three 11-peak features with g values of 2.040, 2.020 and 2.002 (Clozel *et al.*, 1994, 1995). It is probably associated with (deprotonated) surface oxygen atoms on the octahedral sheet (Allard & Calas, 2009).

The present paper describes the EPR spectra of an additional free-radical centre which has been observed in Thai kaolins. This was seen initially in natural (unpurified) kaolin samples that had been subjected to

* E-mail: bernard_a_goodman@yahoo.com
DOI:10.1180/claymin.2016.051.5.01

© 2016 The Mineralogical Society
https://doi.org/10.1180/claymin.2016.051.5.01 Published online by Cambridge University Press

additional doses of γ radiation (Worasith *et al.*, 2013), and was referred to tentatively as the C-centre. It is now shown to correspond to a paramagnetic defect in the kaolin mineral (probably kaolinite) structure, and its X-band EPR spectral characteristics are described here.

EXPERIMENTAL

Kaolin samples

The Lampang kaolin was obtained from the Ban Sa District, Jae Hom, Lampang, and is composed of weathering products of rhyolite in siltstone, sandstone and shale (Kuentag & Wasuwanich, 1978); samples from this deposit contain quartz as a significant impurity. The Ranong kaolin was obtained from the Had Som Pan District, Muang, Ranong, Thailand, and is believed to have been formed by the hydrothermal alteration of granite (Kuentag & Wasuwanich, 1978). It contains both kaolinite and halloysite as kaolin minerals along with some quartz and illite impurities (Worasith *et al.*, 2011). Initially, both kaolin samples were washed with distilled water and dried in an oven at 100°C for 24 h. They were then fractionated by repeated suspension in water (purified by reverse osmosis) and the finest fractions used for the measurements reported here. It should be noted that sedimentation of the Ranong sample, which is dominated by halloysite with a 'needle-like' morphology, was much more rapid than for the Lampang sample which contained 'platy' kaolinite structures.

Radiation treatment

Irradiation of samples to received doses of 100 kGy was performed with γ radiation from a Co-60 source, the main emissions of which are in the MeV energy range. The source was housed in a Gammacell 220 SN 189R (MDS Nordion, Canada) (source activity 220.7 TBq) at the Office of Atoms for Peace, Bangkok, and the received dose rate for the samples was 2.0 Gy/s.

EPR spectroscopy

The EPR spectra were recorded with a Bruker A300 X-band spectrometer, which used a Gunn diode as microwave source and incorporated a high-sensitivity cavity. Individual spectra were recorded over scan ranges of 500 and 30 mT to observe the signals originating from transition metal ions and free radicals, respectively; the latter were obtained as both 1st and 2nd derivatives. Details of additional spectra and all other acquisition parameters are given in the captions for the relevant figures. The g values were calculated by reference to the Bruker ER4119HS-2100 marker accessory which has a g value of 1.9800. Spectral data were processed using the Bruker *WinEPR* software; with samples recorded with the same values for the microwave power, modulation amplitude, time constant and conversion time, intensities were determined both from double integration of complete spectra after background correction, and the heights of individual peaks, and corrected for any differences in the receiver gain or number of scans. Simulations of spectra to test the validity of various models for the C-centre spectrum were performed using the Bruker *SimFonia* software.

RESULTS

Untreated kaolin specimens

The wide-scan EPR spectra of the Lampang and Ranong kaolin specimens (not shown) were similar to those reported by Worasith & Goodman (2012) for unfractionated samples of these minerals. Both contained signals that can be assigned to paramagnetic ions of Fe and Mn; the low-field Fe(III) peaks were considerably broader in the Lampang kaolin than in the Ranong sample, and thus consistent with a more disordered structure, but these signals are not considered further in the present study. The EPR spectrum of the free-radical region of the fine fraction of the Lampang kaolin is shown in Fig. 1a. Signals that correspond to the A- and A′-centres are clearly visible with $g_{//}$ values of 2.050 and 2.036, respectively, and a composite $g_{\perp}$ value of 2.0079. A similar result was also obtained with the Ranong sample, although the A′-centre was weaker and could not be identified conclusively. In addition, both samples contained an easily saturated signal with $g_{//} = 2.0025$ and $g_{\perp} = 2.0013$, which could only be resolved in spectra recorded with low microwave powers and modulation amplitudes. This latter signal probably corresponds to the quartz E′-centre, which is associated with oxygen vacancies (Yip & Fowler, 1975). It was much stronger in the natural Lampang than the natural Ranong sample, as was the relative level of quartz seen in the XRD patterns of these samples (our unpublished results), and although it was much weaker in the fine fractions than in the natural samples or coarse fractions, it was not completely absent even after extensive purification by sedimentation. In addition, there were several poorly resolved features overlapping those from the A- and A′-centres in the natural Lampang sample, but these were lost on

https://doi.org/10.1180/claymin.2016.051.5.01 Published online by Cambridge University Press

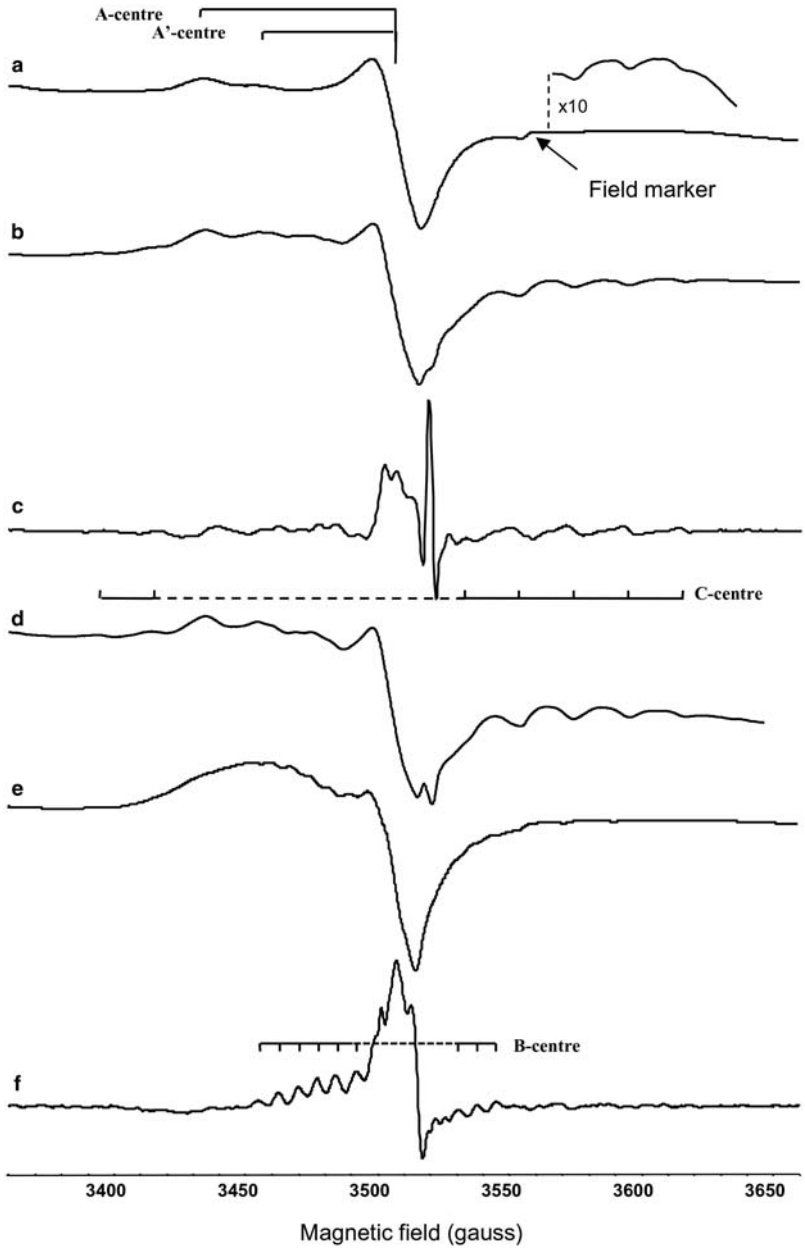

FIG. 1. EPR spectra of the free-radical region of purified kaolin samples. Lampang kaolin 1st derivative of the microwave absorption: (a) before irradiation; (b) after receiving a 100 kGy dose of γ radiation from a ^{60}Co source; and (c) 2nd derivative of the irradiated sample; and (d) spectrum b after subtraction of spectrum a. Ranong kaolin after receiving a 100 kGy dose of γ radiation from a ^{60}Co source recorded as (e) 1st derivative and (f) 2nd derivative. Spectra were recorded in 1024 points using 100 kHz modulation frequency and the following acquisition parameters: 5 mW microwave power, 5 gauss modulation amplitude, 40.96 ms time constant and conversion time.

https://doi.org/10.1180/claymin.2016.051.5.01 Published online by Cambridge University Press

purification of the mineral, and thus probably correspond to the $SiOO^{\cdot}$ centre in quartz (Rink & Odom, 1991), as this was the major impurity in the untreated mineral. Also, as reported previously by Worasith *et al.* (2011), the Ranong sample contained some weak peaks in similar positions to part of the B-centre.

Irradiated kaolin specimens

Major changes were induced in the free-radical region of the EPR spectra of these minerals after exposure to γ radiation, and the results for purified specimens of each mineral after receipt of 100 kGy are shown as 1st and 2nd derivatives in Fig. 1b,c and e,f, along with a difference spectrum between irradiated and unirradiated fine fractions of Lampang kaolin in Fig. 1d to illustrate more clearly the radiation-induced signal. Firstly, note that the changes induced by irradiation are distinctly different for the two kaolins, although overall the spectra of both mineral samples show the generation of substantial quantities of both the B- and C-centres, and both of these centres contain some ^{27}Al hfs. However, the C-centre is the major radiation-induced component in the spectra from the Lampang sample, whereas the B-centre dominates the Ranong spectra. There was some increase in the intensity of the A-centre as a result of irradiation, but it was difficult to assess whether that was also the case with the A′-centre, because of its minor presence and the overlap of its spectrum with those of other components. Nevertheless, overall the C-centre in the Lampang sample, and the B-centre in the Ranong sample were the major radiation-induced products.

In addition to its observation in the irradiated kaolin samples, expansion of the high-field region of the purified, but unirradiated, Lampang sample (Fig. 1a) showed the presence at low intensity of the three highest field peaks from the C-centre, although these were not observed in the spectrum of the Ranong sample.

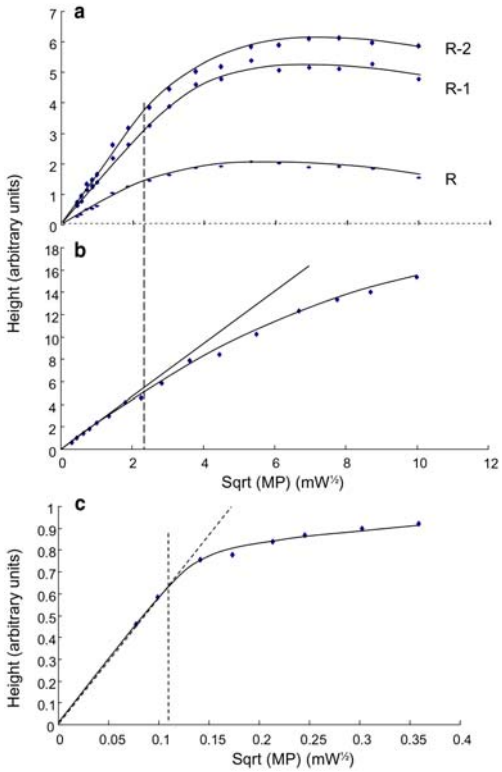

FIG. 2. Plots of signal height *vs.* the square root of the microwave power for: (a) the three highest field peaks of the C-centre radical in the irradiated Lampang kaolin (labelled as R, R-1 and R-2 from the high-field side of the spectrum); (b) the $g_{\perp}$ feature in the unirradiated Lampang kaolin (which is derived primarily from the A-centre); and (c) the putative E′ signal from quartz in the unpurified Lampang sample.

Saturation characteristics of the C-centre

Although many of the peaks of the C-centre overlap with other components in the spectra, two peaks on the low-field side and four peaks on the high-field side of the spectrum of the A-centre are resolved. Of these, the three peaks at the highest field values are largely free from interference from other radicals in the spectra, apart from some overlap with the 4th peak of the relatively broad Mn spectrum. Measurements of their intensities after irradiation of the purified Lampang sample were performed on the basis of their heights in 1st (Fig. 2a) and 2nd derivative recordings (not shown) and then plotted as a function of the square root of the microwave power to construct saturation curves. For comparison, saturation curves for the A-centre (from the unirradiated Lampang sample) and the quartz E′-centre in the unpurified Lampang kaolin are shown in Fig. 2b,c, respectively. These results show clearly that the A- and C-centres have similar saturation characteristics, and that saturation commences at ~5 mW microwave power with the high-sensitivity cavity used for the current measurements. Because of signal overlap, it was not possible to produce reliable saturation curves for the A′- and B-centres, but the results are consistent with values being similar to those of the A- and C-centres. However, the saturation characteristics of the quartz E′-centre (Fig. 2c) are

https://doi.org/10.1180/claymin.2016.051.5.01 Published online by Cambridge University Press

completely different from those of the other radical centres in these samples, and saturation commenced at ~11 μW.

Stability of the C-centre

The effect of heating to 300°C on the EPR spectrum of the purified Lampang kaolin that had been irradiated with a 100 kGy dose is shown in Fig. 3. The peaks associated with the A′- and C-centres were lost, whilst those associated with the A-centre were increased in intensity, although overall ~30% of the total radical signal intensity was decreased as a result of heating to 300°C. A detailed investigation of the stability of the radiation-induced paramagnetic centres in these Thai kaolins is the subject of a separate, more detailed investigation (Worasith *et al.,* unpublished results), but the decrease in intensity of the C-centre resonance was progressive in the temperature range 150–270°C.

Spin Hamiltonian parameters for the C-centre radical

Determination of the EPR spectral parameters for the C-centre is not unambiguous, because the entire central region overlaps with features from other components in the spectra. By subtracting the spectrum of the unirradiated sample that had been heated to 300°C from that of the irradiated but unheated Lampang sample (Fig. 1b), it was possible to generate an approximate spectrum for the C-centre radical for more detailed analysis, although it must be recognized that this difference spectrum also contains contributions from any other spectral components that are altered by heating. Three possible scenarios are considered below, namely an isotropic spectrum, a spectrum with axial symmetry, and one with orthorhombic symmetry.

(i) A single isotropic spectrum. The positions of the peaks at the low- and high-field ends of the spectrum (Fig. 4a) correspond roughly to the positions expected for the extreme peaks in an 11-peak spectrum such as would occur for interaction of an unpaired electron with two equivalent ^{27}Al (I = 5/2) nuclei; a simulation of such a spectrum is shown in Fig. 4b with g = 2.0088 and A(^{27}Al) = 2.15 mT. On comparing the experimental and simulated spectra, it can be seen that although there is an approximate correspondence to the 1:2:3:4:5:6:5:4:3:2:1 intensity ratio in the simulation, the experimental peaks have 'absorption-like' shapes typical of the extreme features in anisotropic spectra, and are not characteristic of isotropic spectra.

(ii) An axially symmetric spectrum. The positions and separations of the experimental peaks could, in principle, correspond to the extreme features associated with the $g_{//}$ and $g_{\perp}$ components of an axially symmetric spectrum (*i.e*. comparable to the A- and A′-centres, but with interaction of the unpaired electron with a single ^{27}Al nucleus). Simulations with peaks in the positions of those observed in the experimental spectrum are shown in Fig. 4c for $g_{//} = 2.0417$, $g_{\perp} = 1.9765$, $A_{//} = A_{\perp} = 2.10$ mT, and Fig. 4d for $g_{//} = 1.976$, $g_{\perp} = 2.041$, $A_{//} = A_{\perp} = 2.10$ mT. However, the relative intensities of the low- and high-field peaks in these simulations are not consistent with the experimental spectrum.

(iii) A spectrum corresponding to orthorhombic symmetry. Such a spectrum would consist of three separate g values, each with sextet hyperfine structure from interaction of the unpaired electron with a single ^{27}Al nucleus. Reasonable parameters for the high- and low-field, g_1 and g_3, components can be obtained by reproducing the positions of the experimental peaks, but determination of the g_2 value is not unambiguous. A simulation based on $g_1 = 1.976$, $g_2 = 2.01$, $g_3 = 2.0417$, $A_1(^{27}Al) = A_2(^{27}Al) = A_3(^{27}Al) = 2.10$ mT is shown in Fig. 4e, and this reproduces reasonably well the positions and shapes of the experimental peaks at the low- and high-field ends of the spectrum (although the highest field peak is weaker in the experimental than in the simulated spectrum). However, reasonable simulations could also be achieved with g_2 values in the range 2.00–2.20. In addition, the experimental spectrum provides no information on the magnitude of $A_2(^{27}Al)$ although it is likely to be close to those of A_1 and A_3, as in the B-centre. It should also be noted that the experimental spectrum contains additional intensity in its central region, but this probably corresponds to contributions from the A′- and B-centres, which are also unstable under heating. Also, the sharp peak at ~3523 gauss in Fig. 4a probably corresponds to a thermally unstable radiation-induced signal in the quartz impurity. Overall, on the basis of these simulations, a signal consistent with orthorhombic symmetry is considered the most likely interpretation of the C-centre spectrum. However, it should be possible to obtain more definitive parameters if spectra could be recorded on additional spectrometers operating at different microwave frequencies.

https://doi.org/10.1180/claymin.2016.051.5.01 Published online by Cambridge University Press

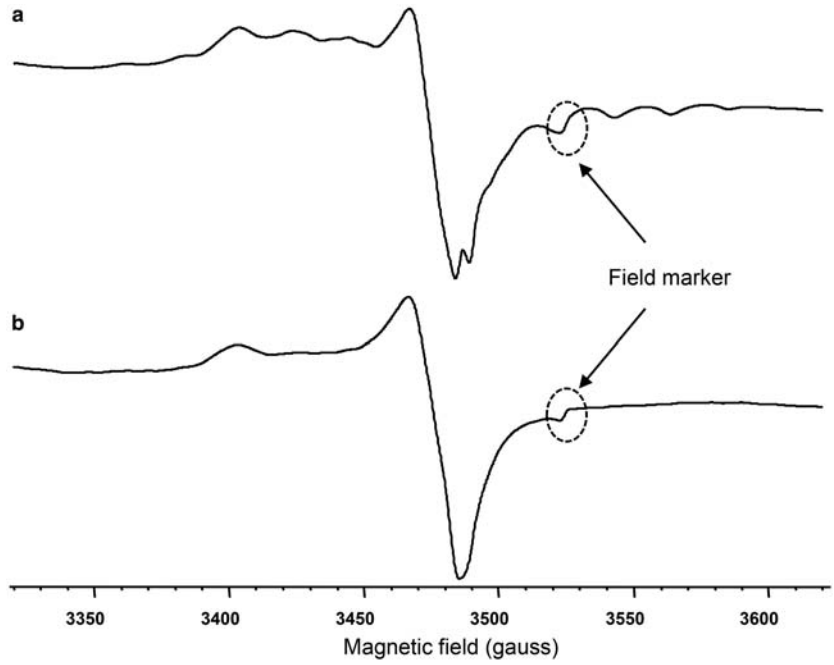

FIG. 3. 1st derivative recordings of the free-radical region of the EPR spectra of a purified sample of the Lampang kaolin: (a) before; and (b) after heating at 300°C for 1 h. Acquisition parameters are: 2048 points, 5 mW microwave power, 5 gauss modulation amplitude, 40.96 ms time constant and conversion time.

DISCUSSION

The radiation-induced C-centre described here has not been reported previously for kaolin samples from other parts of the world. Therefore, an initial consideration had to be whether it is actually associated with one or more of the kaolin minerals, or an impurity phase. Because the Lampang sample represents the main source of the C-centre, the discussion focuses on this kaolin sample, which actually contained significant quantities of quartz as an impurity in the original deposit. Indeed, the EPR spectrum of the free radical region of the crude Lampang kaolin sample before irradiation (Worasith & Goodman, 2012) closely resembles those reported for quartz grains isolated from granite or rhyolite samples at 10 mW microwave power by Rink & Shimoyama (1991). However, purification of the kaolin by repeated sedimentation, which was designed to remove denser impurity phases, such as quartz, did not result in any decrease in the contribution of the C-centre to the EPR spectra of irradiated samples, whereas the fine fraction showed a large reduction in the contribution of spectral components associated with quartz compared to the natural sample and coarse fractions separated from the same bulk specimen. Furthermore, the saturation characteristics of the C-centre are distinctly different from those of the quartz-based E′-centre, which saturated easily and is only fully resolved at low microwave power and modulation amplitude. The other impurity identified in the kaolin samples with which the C-centre could possibly be associated is illite. Although this assignment cannot be excluded definitively, Morichon *et al.* (2008) found that the radiation-induced paramagnetic centre in illites has EPR spectra that resemble the A′-centre ($g_{//} = 2.032$, $g_{\perp} = 1.993$), but with no saturation at microwave powers as high as 200 mW. Consequently, it is unlikely that the C-centre in our Thai samples originates from an illite impurity, or at least from an illite sample with similar composition to that studied by Morichon *et al*. However, as with most aluminosilicate minerals, illites can have a range of compositions, and we cannot conclude with absolute certainty that it is not possible to form a paramagnetic centre with parameters similar to the C-centre in some illite with a special composition, although there is no evidence for this in either the present or published works. Therefore, the two main crystalline impurities

https://doi.org/10.1180/claymin.2016.051.5.01 Published online by Cambridge University Press

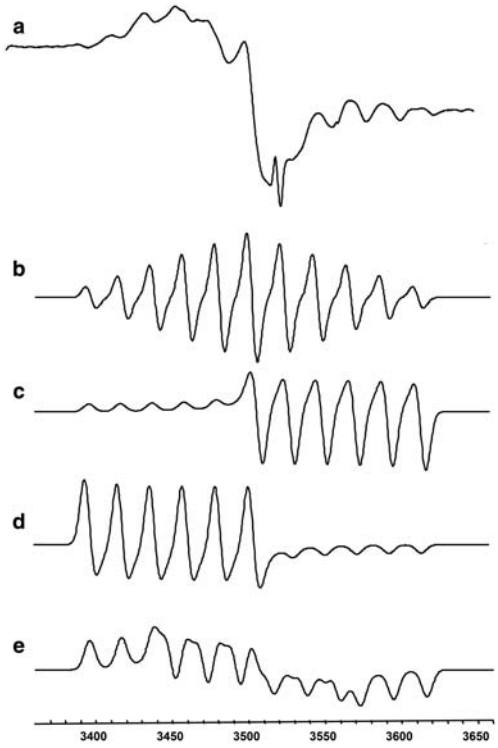

FIG. 4. (a) EPR spectrum of a signal in irradiated Lampang kaolin (Fig. 1b) after subtracting the signal that remained after heating to 300° (Fig. 3b), along with simulations for an isotropic signal with g = 2.0088 and two equivalent ^{27}Al atoms with A(^{27}Al) = 2.15 mT (b), axially symmetric signal with $g_{//} = 2.0417$, $g_{\perp} = 1.9765$, $A_{//} = A_{\perp} = 2.10$ mT (c), axially symmetric signal with $g_{//} = 1.976$, $g_{\perp} = 2.041$, $A_{//} = A_{\perp} = 2.10$ mT (d), and a rhombic signal with $g_1 = 1.976$, $g_2 = 2.01$, $g_3 = 2.0417$, $A_1 = A_2 = A_3 = 2.10$ mT (e).

in the kaolin minerals are unlikely to be the source of the C-centre radical. Very fine particles of poorly crystalline minerals that could have escaped detection by XRD must also be considered as a possible source of the C-centre. However, such particles would be expected to be concentrated in the fine fraction, whereas the C-centre resonance was detected at similar levels in all fractions (unpublished results). In addition, small particles of poorly crystalline minerals are less likely to stabilize radical centres than crystalline samples, but, as shown in Fig. 1, the C-centre represents the main radiation-induced product from the Lampang kaolin. Therefore, by a process of elimination of alternative explanations, it is highly probable that the C-centre is associated with one or more of the kaolin-group minerals.

As described by Allard & Calas (2009), the A-, A′-, and B-centres all correspond to O^- ions formed by ejection of an electron from O^{2-} in the aluminosilicate structure, and their different EPR spectra are determined by the specific sites at which these defects are located. The high degree of anisotropy in the g values in the EPR spectrum of the C-centre is also consistent with it being based on an O^- centre, and the ^{27}Al hyperfine structure indicates that it is adjacent to a single aluminium atom. Also, the spectral simulations show that this ^{27}Al atom has a much larger hfs than that observed for the two equivalent ^{27}Al atoms in the B-centre spectrum, and thus indicates that the B- and C-centres are associated with different types of structural site. Nevertheless, the magnitude of this ^{27}Al hyperfine structure shows that the amount of unpaired electron density on the Al is still probably quite small, although, without values for the anisotropic contribution, it is not possible to estimate its value.

As shown in Fig. 3, the C-centre is not stable to heating to 300°C, and the loss of its signal intensity was accompanied by an increase in intensity of the A-centre. Although this result suggests that the C-centre could be transformed to the A-centre, there was also a large change in the Q-value of the resonator cavity as a result of heating the sample, and the quantitative nature of heat-induced changes in these paramagnetic centres is the subject of a more detailed investigation.

CONCLUSIONS

Investigations by EPR of kaolins from the two main deposits in Thailand have revealed the production of a paramagnetic centre that has not been described in kaolin samples from other parts of the world, and which we refer to here as the C-centre (to distinguish it from the previously reported A-, A′-, and B-centres). This C-centre was the major paramagnetic centre produced by irradiation of the Lampang kaolin, in which kaolinite is the major kaolin mineral, whereas the B-centre radical dominated the EPR spectra of irradiated samples of the Ranong kaolin, where halloysite is the major kaolin mineral. However, the C-centre was observed as a minor component in the irradiated Ranong sample, which also contains some kaolinite, and it is possible that it may be specifically associated with the kaolinite phase. However, results from two deposits are insufficient to draw such general conclusions, especially as similar spectra have not been observed in kaolin minerals from other sources. This lack of observation of a similar resonance in the many reported investigations of the EPR spectra of kaolin

https://doi.org/10.1180/claymin.2016.051.5.01 Published online by Cambridge University Press

minerals is puzzling, and in our work we have only conclusively identified its presence in one other specimen of several different kaolin samples we have studied from various parts of the world. It would appear, therefore, that this resonance is not of universal occurrence in kaolin mineral samples irradiated at ambient temperature, and that it may have some special compositional requirement for its stabilization.

ACKNOWLEDGEMENTS

The authors thank Ms Sumalee Ninlaphruk of the Office of Atoms for Peace, Bangkok, Thailand for performing the sample irradiation. The work was supported by internal funding from the Rajamangala University of Technology Krungthep, Thailand, the National Natural Science Foundations of China (Grant No. 11265002), and the Natural Science Foundations of Guangxi (Grant No. 2010GXNSFD013036).

REFERENCES

Allard Th. & Calas G. (2009) Radiation effects on clay mineral properties. *Applied Clay Science* **43**, 143–149.

Allard Th., Balan E., Calas G., Fourdrin C., Morichon E. & Sorieul S. (2012) Radiation-induced defects in clay minerals: A review. *Nuclear Instruments and Methods in Physics Research Section B*, **277**, 112–120.

Clozel B., Allard T. & Muller J.-P. (1994) Nature and stability of radiation-induced defects in natural kaolinites: new results and a reappraisal of published works. *Clays and Clay Minerals*, **42**, 657–666.

Clozel B., Gaite J.-M. & Muller J.-P. (1995) Al-O-Al paramagnetic defects in kaolinite. *Physics and Chemistry of Minerals*, **22**, 351–356.

Cuttler A.H. (1980) The behaviour of a synthetic ^{57}Fe-doped kaolin: Mössbauer and electron paramagnetic resonance studies. *Clay Minerals*, **15**, 429–444.

Hall P.L. (1980) The application of electron spin resonance spectroscopy to studies of clay minerals: I. Isomorphous substitutions and external surface properties. *Clay Minerals*, **15**, 321–335.

Kuentag C. & Wasuwanich P. (1978) Cljay. *Economic Geology Bulletin* No. **19**. Economic Geology Division, Department of Mineral Resources, Thailand (in Thai).

Lombardi K., Guimarães J.L., Mangrich A.S., Mattoso N., Abbate M., Schreiner W.H. & Wypych F. (2002) Structural and morphological characterization of the PP-0559 kaolinite from the Brazilian Amazon region. *Journal of the Brazilian Chemical Society*, **13**, 270–275.

Morichon E., Allard T., Beaufort D. & Patrier P. (2008) Evidence of native radiation-induced paramagnetic defects in natural illites from unconformity-type uranium deposits. *Physics and Chemistry of Minerals*, **35**, 339–346.

Muller J.-P. & Calas G. (1993) In: *Kaolin Genesis and Utilization* (H.H. Murray, W. Bundy & C. Harvey editors). The Clay Minerals Society, Boulder, Colorado, USA.

Rink W.J. & Odom A.L. (1991) Natural alpha recoil particle radiation and ionizing radiation sensitivities in quartz detected with EPR: implications for geochronometry. *International Journal of Radiation Applications and Instrumentation. Part D. Nuclear Tracks and Radiation Measurements*, **18**, 163–173.

Rink W.J. & Shimoyama Y. (1991) Improved detection of EPR signals used in quartz dating. *Ancient TL*, **9**, 33–36.

Worasith N. & Goodman B.A. (2012) Influence of particle size on the paramagnetic components of kaolins from different origins. *Clay Minerals*, **47**, 539–557.

Worasith N., Goodman B.A., Jeyachoke N. & Thiravetyan P. (2011) Characterisation of modified kaolin from the Ranong deposit Thailand studied by XRD, XRF, SEM, FTIR and EPR. *Clay Minerals*, **46**, 525–545.

Worasith N., Ninlaphruk S., Mungpayaban H. & Goodman B.A. (2013) Irradiation-induced free radicals in Thai kaolins. *Proceedings of the Pure and Applied Chemistry International Conference 2013 (PACCON 2013)*, pp. 294–297.

Yip K.L. & Fowler W.B. (1975) Electronic structures of E1′ centres in SiO2. *Physcial Review B*, **11**, 2327–2328.

https://doi.org/10.1180/claymin.2016.051.5.01 Published online by Cambridge University Press